A. Ankiewicz* and A. Chowdury

Superposition of Solitons with Arbitrary Parameters for Higher-order Equations

DOI 10.1515/zna-2016-0098
Received March 15, 2016; accepted May 30, 2016; previously published online June 23, 2016

Abstract: The way in which solitons propagate and collide is an important theme in various areas of physics. We present a systematic study of the superposition of solitons in systems governed by higher-order equations related to the nonlinear Schrödinger family. We allow for arbitrary amplitudes and relative velocities and include an infinite number of equations in our analysis of collisions and superposed solitons. The formulae we obtain can be useful in determining the influence of subtle effects like higher-order dispersion in optical fibres and small delays in the material responses to imposed impulses.

Keywords: Solitons Superposition Higher-Order Equations Collisions.

PACS Numbers: 05.45.Yv; 42.65.Tg; 42.81.Qb

1 Introduction

The propagation [1] of solitons of the well-known nonlinear Schrödinger equation (NLSE) and their collisions [2] have been the subject of many works. Experiments have verified collision phenomena [3]. When two solitons have the same velocity and have no offset, then 'breathers' can appear. 'Breathers' are nonlinear formations that vary periodically. The periodicity can be in the propagation direction (Ma type), as verified in [4], or in the transverse (Akhmediev type) direction, as observed in fibres in [5]. It can also be at an angle to each axis. These, too, have been analysed in [1] and have also been observed in water [6]. An initial condition with transverse shape sech(t) leads to the propagation of an unchanging soliton, whereas the initial condition 2 sech(t) leads to the propagation of a periodic breather that can be regarded as a 'second-order soliton'.

Recently, some higher-order equations have been considered as well, since they can have various applications, especially to propagation of short pulses in optical fibres. The Hirota equation includes third-order dispersion and a higher-order nonlinear term, so it can be useful in fibre studies. Breather-to-soliton conversion, for a system described by this equation, has been explained in [7]. The Sasa-Satsuma [8] and Hirota equations, and deviations from them, have terms describing third-order dispersion, self-steepening, and self-frequency shift. They have been studied in [9]. A still-higher-order equation, called a quintic equation due to its inclusion of fifth order dispersion, also supports solitons [10], breathers [11], and breather-to-soliton conversions [12].

Due to applications to pulses in optical fibres, wave formations in water and superposed waves in BECs [13], a full investigation is well worthwhile, and here we provide general results that can be useful in various areas of physics. Two relevant recent reviews describing Bose-Einstein condensates are [14] and [15].

The basic Kerr effect, i.e., cubic nonlinearity, leads to the ubiquitous NLSE, and this then delineates nonlinear formations in fibres and water. However, this is not an exact representation of reality, since both fibres and water waves exhibit deviations from NLSE pulses. In fact, an infinite number of higher-order nonlinear Schrödinger-type operators can be written down [16]. The full equation then can allow for higher orders of dispersion and nonlinearity, thus going well beyond the Kerr effect. Hence, a wider range of physical systems can be represented by adding combinations of these operators, to form a single equation with many terms. The full system still supports solitons, breathers, and rogue waves. In this article, we seek an understanding of the propagation of colliding solitons of the full system and especially the behaviour of superimposed solitons. In the reverse direction, measurement of deviations from NLSE pulses (in water, fibres, plasma, etc.) could be used to determine the nature and form of the physical effects causing those deviations.

We consider an equation that includes an infinite number of functionals, where each has an arbitrary coefficient. The whole infinite hierarchy is thus expressed:

***Corresponding author: A. Ankiewicz,** Optical Sciences Group, Research School of Physics and Engineering, The Australian National University, Canberra ACT 2600, Australia, Tel.: +02 6125 0000, E-mail: Adrian.Ankiewicz@anu.edu.au
A. Chowdury: Optical Sciences Group, Research School of Physics and Engineering, The Australian National University, Canberra ACT 2600, Australia, E-mail: Amdadul.Chowdury@anu.edu.au

$$F[\psi(x,\,t)]=i\psi_x+\sum_{j=1}^{\infty}(\alpha_{2j}K_{2j}-i\alpha_{2j+1}K_{2j+1})=0, \tag{1}$$

where each functional, K_p, depends on $(x,\,t)$, and each coefficient, α_p, $p=2,\,3,\,4,\,5,\,\ldots,\,\infty$ is an arbitrary real number. In all expressions here, x is the propagation variable and t is transverse variable (time in a moving frame), with the function $|\psi(x,\,t)|$ being the envelope of the waves. Using one equation containing many functionals allows us to describe common and uncommon physical effects in fibres, water, and other systems. This then includes terms with low- and high-order derivatives in t.

The book [1] and many papers use $\alpha_2=\frac{1}{2}$, but it can take any value, including zero.

A general method, using a recurrence relation, to obtain each particular operator K_n, is given in [16]. For convenience, we present the first few operators.

$$K_2[\psi(x,\,t)]=\psi_{tt}+2\psi|\psi|^2. \tag{2}$$

Clearly, $i\psi_x+\alpha_2K_2=0$ is the basic NLSE. Then

$$K_3[\psi(x,\,t)]=\psi_{ttt}+6|\psi|^2\psi_t. \tag{3}$$

If α_3 is nonzero, but all other α_j's are zero, then (1) reduces to the basic Hirota equation.

Next,

$$K_4[\psi(x,\,t)]=\psi_{tttt}+8|\psi|^2\psi_{tt}+6\psi|\psi|^4+4\psi|\psi_t|^2+6\psi_t^2\psi^*+2\psi^2\psi_{tt}^*. \tag{4}$$

If α_4 is nonzero, but all other α_j's are zero, then (1) reduces to the 'LPD' equation.

Finally,

$$K_5[\psi(x,\,t)]=\psi_{ttttt}+10|\psi|^2\psi_{ttt}+10(\psi|\psi_t|^2)_t+20\psi^*\psi_t\psi_{tt}+30|\psi|^4\psi_t. \tag{5}$$

If α_5 is nonzero, but all other α_j's are zero, then (1) reduces to the 'quintic' equation.

Thus, the first term in each K_p is the t derivative of ψ of order p, viz. the dispersion of order p.

2 Simple Expression for Single Soliton with Complex Parameter

We allow for an arbitrary parameter and seek a soliton solution that includes infinitely many operators. We thus define $\lambda=a+ib$. The real part, a, controls velocity, whereas the imaginary part, b, controls amplitude. We use the ansatz:

$$\psi=2b\,e^{-2i(at+\phi_a x)}\,\mathrm{sech}[2b(t+v_k x)] \tag{6}$$

where the terms can be expressed directly in terms of λ and its conjugate, λ^*. We can determine the contribution from each α_p separately and then add them to get the result that includes many contributions. The pattern thus revealed then allows us to present closed-form general solution and check its validity. For integer n, $(n=2,\,3,\,\ldots\,\cdots)$, we define

$$f(n)=\Big[\mathrm{mod}(n+3,\,4)-\mathrm{mod}(n+1,\,4)\Big]/2=\sqrt{2}\cos\left[(2n+1)\frac{\pi}{4}\right].$$

Hence $f(2)=-1$, $f(3)=1$, $f(4)=1$, etc.

We have

$$\begin{aligned}\phi_a&=-\sum_{n=2}^{\infty}2^{n-2}f(n)\alpha_n[\lambda^n+(\lambda^*)^n]\\&=2(a^2-b^2)\alpha_2-4a(a^2-3b^2)\alpha_3\\&\quad-8(a^2-2ab-b^2)(a^2+2ab-b^2)\alpha_4\\&\quad+16a(a^4-10a^2b^2+5b^4)\alpha_5\\&\quad+32(a-b)(a+b)(a^2-4ab+b^2)(a^2+4ab+b^2)\alpha_6\\&\quad-64a(a^6-21a^4b^2+35a^2b^4-7b^6)\alpha_7+\cdots,\end{aligned}$$

and

$$\begin{aligned}v_k&=\frac{i}{b}\sum_{n=2}^{\infty}2^{n-2}f(n)\alpha_n[\lambda^n-(\lambda^*)^n]\\&=4a\alpha_2-4(3a^2-b^2)\alpha_3-32a(a^2-b^2)\alpha_4\\&\quad+16(5a^4-10a^2b^2+b^4)\alpha_5+64a(a^2-3b^2)(3a^2-b^2)\alpha_6\\&\quad-64(7a^6-35a^4b^2+21a^2b^4-b^6)\alpha_7+\cdots.\end{aligned}$$

3 Second-order Solitons

3.1 Distinct Parameters

We now consider second-order solitons, i.e. cases where the 'launch' $(x=0)$ condition is a soliton of twice the basic soliton amplitude, viz. $2c\,\mathrm{sech}(ct)$, where c is arbitrary. Results of the previous section suggest that we can use the basic NLSE solution (e.g. see eq. 3.81 of [1]), with α_2 not restricted to being 1/2, as an ansatz and then modify velocities, phases, and 'stretching factors' according to the contributions found for each individual functional form (with coefficient α_p) in the full equation. Again, the determination of individual components indicates the final, relatively simple, form of these velocities, etc.

The general solution, for any number of operators in the hierarchy, is

$$\psi=4c\frac{e^{ix\phi_y}\cosh[3c(t+v_b x)]+3e^{ixB_z}\cosh[c(t+v_a x)]}{\cosh[4c(t+v_c x)]+4\cosh[2c(t+v_d x)]+3\cos[B_y x]}, \quad (7)$$

where

$$v_a=\sum_{n=1}^{\infty}\alpha_{2j+1}c^{2j}, \quad (8)$$

$$v_b=\sum_{n=1}^{\infty}\alpha_{2j+1}(3c)^{2j}, \quad (9)$$

while $v_c=\frac{1}{4}(3v_b+v_a)$ and $v_d=\frac{1}{2}(3v_b-v_a)$. The coefficients relevant for the even terms are as follows:

$$\phi_y=\sum_{n=1}^{\infty}\alpha_{2j}c^{2j}, \quad (10)$$

$$B_z=\sum_{n=1}^{\infty}\alpha_{2j}(3c)^{2j}, \quad (11)$$

while $B_y=B_z-\phi_y$. In all cases, $\psi(0, t)=2c\,\mathrm{sech}(ct)$, indicating that we have a second-order soliton. If $\alpha_2=1/2$ and all other α_j's are zero, then this result reduces to the known NLSE result [1]. For an equation consisting of only even order operators, the pattern is of a propagation field which remains close to $t=0$. For $t=0$, the oscillation has a maximum value of $|\psi(x, 0)|_{\max}=4c$ and a minimum value of $|\psi(x, 0)|_{\min}=2c$. An example is plotted in Figure 1; it resembles fig. 3.16 of [1]. For an equation consisting of only odd-order operators, the initial condition creates two solitons, one of which stays close to $t=0$, while the other propagates on a tilt, i.e. it has nonzero velocity. An example is plotted in Figure 2; in these cases, for each soliton, the 'collision' at $x=0$ just causes a lateral offset.

3.2 Two-soliton Breather

We now study nonlinear interference by setting the velocities a_1 and a_2 to 0. Here, the general solution, for real $b_1\neq b_2$, is

$$\psi=4(b_2^2-b_1^2)\frac{T}{L}, \quad (12)$$

where

$$T=b_1e^{ix\phi_g}\cosh[2b_2(t+w_b x)]-b_2e^{ixB_g}\cosh[2b_1(t+w_a x)]$$

and

$$L=(b_1-b_2)^2\cosh[2(b_1+b_2)(t+w_c x)]+(b_1+b_2)^2\cosh[2(b_2-b_1)(t+w_d x)]-4b_1b_2\cos[B_d x],$$

where

$$w_a=\sum_{n=1}^{\infty}\alpha_{2j+1}(2b_1)^{2j}, \quad (13)$$

$$w_b=\sum_{n=1}^{\infty}\alpha_{2j+1}(2b_2)^{2j}, \quad (14)$$

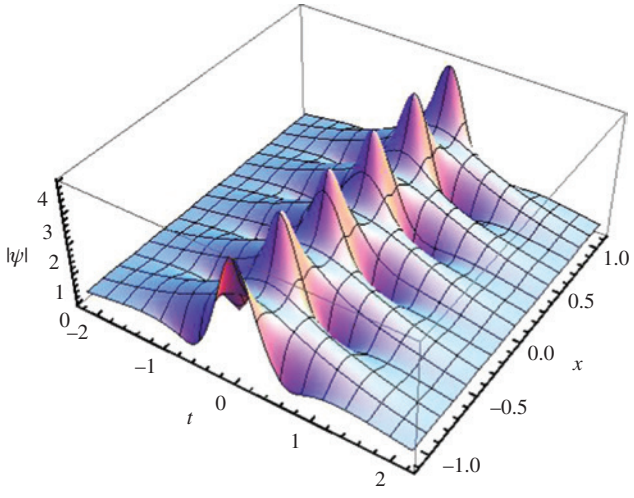

Figure 1: Plot of breather, (7), using $c=1$, $\alpha_2=1/2$, $\alpha_4=1/8$, with all other α_j's being zero. For $t=0$, the amplitude ranges from 2 to 4.

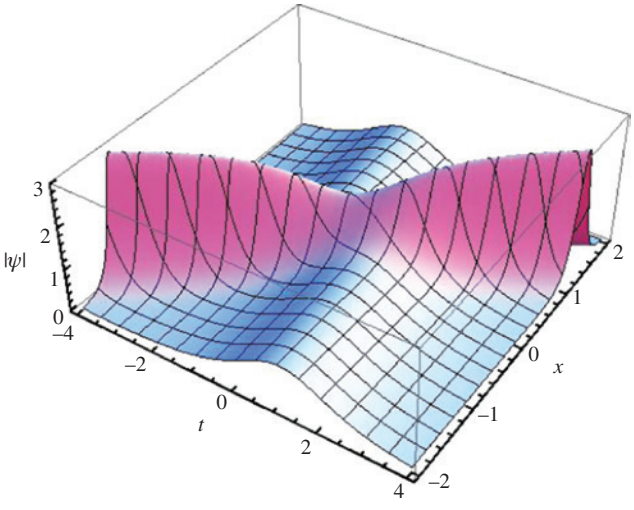

Figure 2: Plot of breather, (7), using $c=1$, $\alpha_3=1/4$, $\alpha_5=-1/16$, with all other α_j's being zero.

while $w_c=\frac{b_1w_a+b_2w_b}{b_1+b_2}$ and $w_d=\frac{b_1w_a-b_2w_b}{b_1-b_2}$. The coefficients relevant for the even terms are as follows:

$$\phi_g=\sum_{n=1}^{\infty}\alpha_{2j}(2b_1)^{2j}, \tag{15}$$

$$B_z=\sum_{n=1}^{\infty}\alpha_{2j}(2b_2)^{2j}, \tag{16}$$

while $B_d=B_g-\phi_g$.

The maximum value is $|\psi(0,0)|=2|b_1+b_2|$. If $\alpha_2=1/2$ and all other α_j's are zero, then this result reduces to the known NLSE result (e.g. see eq. 3.79 of [1]). For an equation consisting of only even order operators, the pattern is of a propagation field, with periodic peaks, which remains close to $t=0$, so it resembles fig. 3.14 of [1]. We give an example, using $b_1=1$, $b_2=3/2$, with $\alpha_4=1/4$ and all other α_j's being zero in Figure 3.

3.3 Complex Equal Parameters

We now allow for complex parameters and seek a multi-soliton solution with zero-phase difference between components. We set $a_1=-a_2=a$, $b_1=b_2=b$, so the amplitudes are equal and velocities are opposite. We can thus define $\lambda=a+ib$. We get

$$\psi=-8iab\frac{A(x,t)+iB(x,t)}{D(x,t)}e^{-2ikx+i(\varphi_1+\varphi_2)}$$

where

$$\begin{aligned}A(x,t)=&\cosh(hx)\{a\cos[2a(t+4w_5x)+\Delta\varphi]\cosh[2b(t+4v_5x)]\\&-b\sin[2a(t+4w_5x)+\Delta\varphi]\sinh[2b(t+4v_5x)]\},\\B(x,t)=&\sinh(hx)\{a\sin[2a(t+4w_5x)+\Delta\varphi]\sinh[2b(t+4v_5x)]\\&+b\cos[2a(t+4w_5x)+\Delta\varphi]\cosh[2b(t+4v_5x)]\},\\D(x,t)=&(a^2+b^2)\cosh(2hx)+a^2\cosh[4b(t+4v_5x)]\\&-b^2\cos[4a(t+4w_5x)+2\Delta\varphi].\end{aligned}$$

Here, the phase difference between the two solitons is $2\Delta\varphi=2(\varphi_1-\varphi_2)$. Interestingly, the terms can be expressed directly in terms of λ and its conjugate, λ^*. The (real) coefficients relevant to even order operators are as follows:

$$\begin{aligned}k=&-\sum_{j=1}^{\infty}2^{2j-2}\alpha_{2j}(-1)^j[\lambda^{2j}+(\lambda^*)^{2j}]\\=&2\alpha_2(a^2-b^2)-8\alpha_4(a^4-6a^2b^2+b^4)\\&+32\alpha_6(a^6-15a^4b^2+15a^2b^4-b^6)\\&-128\alpha_8(a^8-28a^6b^2+70a^4b^4-28a^2b^6+b^8)+\cdots,\end{aligned}$$

and

$$\begin{aligned}h=&i\sum_{j=1}^{\infty}2^{2j-1}\alpha_{2j}(-1)^j[\lambda^{2j}-(\lambda^*)^{2j}]\\=&4ab[2\alpha_2-16\alpha_4(a-b)(a+b)+32\alpha_6(3a^4-10a^2b^2+3b^4)\\&-512\alpha_8(a^6-7a^4b^2+7a^2b^4-b^6)+512\alpha_{10}(5a^8-60a^6b^2\\&+126a^4b^4-60a^2b^6+5b^8)+\cdots]\end{aligned}$$

The (real) coefficients relevant to odd order operators are as follows:

$$\begin{aligned}w_5=&\frac{1}{2a}\sum_{j=1}^{\infty}2^{2j-2}\alpha_{2j+1}(-1)^j[\lambda^{2j+1}+(\lambda^*)^{2j+1}]\\=&-(a^2-3b^2)\alpha_3+4\alpha_5(a^4-10a^2b^2+5b^4)\\&-16\alpha_7(a^6-21a^4b^2+35a^2b^4-7b^6)+\cdots,\end{aligned}$$

and

$$\begin{aligned}v_5=&-\frac{i}{2b}\sum_{j=1}^{\infty}2^{2j-2}\alpha_{2j+1}(-1)^j[\lambda^{2j+1}-(\lambda^*)^{2j+1}]\\=&-(3a^2-b^2)\alpha_3+4\alpha_5(5a^4-10a^2b^2+b^4)\\&-16\alpha_7(7a^6-35a^4b^2+21a^2b^4-b^6)+\cdots.\end{aligned}$$

If we set $\alpha_2=1/2$ and all other operator coefficients to zero, this form reduces to the known NLSE collision of two solitons with equal amplitudes (see e.g. eq. 3.78 of [1]).

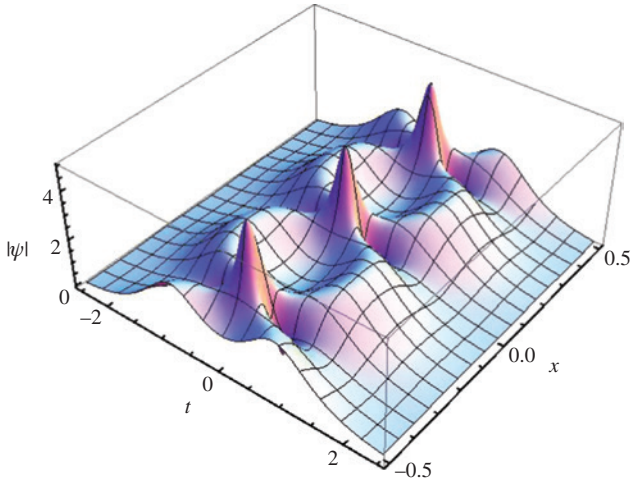

Figure 3: Plot of breather, (12), using $b_1=1$, $b_2=3/2$, with $\alpha_4=1/4$ and all other α_j's being zero. Here the maximum amplitude is 5.

4 Complex Arbitrary Parameters

We now allow for arbitrary parameters and seek a multi-soliton solution that includes infinitely many operators. We thus define $\lambda_m = a_m + ib_m$, $m=1, 2$. The real parts control velocities, while the imaginary parts control amplitudes. We allow a_1, a_2, b_1, b_2, and all the α_j's to be arbitrary. We find

$$\psi = 2\frac{N_2(x,t)}{D_2(x,t)}e^{-2i(\Omega_1+\Omega_2)} \tag{17}$$

where

$$\begin{aligned} N_2(x,t) &= ib_2\cosh(2\Theta_1)e^{2i\Omega_1(x,t)}[(a_1-a_2)^2-b_1^2+b_2^2] \\ &+ ib_1\cosh(2\Theta_2)e^{2i\Omega_2(x,t)}[(a_1-a_2)^2+b_1^2-b_2^2] \\ &-2b_1b_2(a_1-a_2)S_1(x,t), \end{aligned}$$

and

$$D_2(x,t) = [(a_1-a_2)^2+b_1^2+b_2^2]S_2(x,t) - 2b_1b_2S_3(x,t).$$

Now the S_j are defined as follows:

$$\begin{aligned} S_1(x,t) &= e^{2i\Omega_1(x,t)}\sinh(2\Theta_1) - e^{2i\Omega_2(x,t)}\sinh(2\Theta_2), \\ S_2(x,t) &= \cosh(2\Theta_1)\cosh(2\Theta_2), \\ S_3(x,t) &= \cos[2(\Omega_1(x,t)-\Omega_2(x,t))] + \sinh(2\Theta_1)\sinh(2\Theta_2), \end{aligned}$$

where $\Omega_m(x,t)$ and $\Theta_m(x,t)$ are given as (25) to (26) in the Appendix. All the coefficients are given in the Appendix.

In fact, the coefficients can be simplified. We define a single factor, $\phi_m = k_m + 4a_m w_m$ and also $b_m y_m = h_m/2 + 4b_m v_m$, $m=1, 2$. Hence, we can now replace (25)–(30) of the Appendix with the following:

$$\Omega_m(x,t) = a_m t + x\phi_m,$$

and

$$\Theta_m(x,t) = b_m(t + xy_m),$$

where

$$\begin{aligned} \phi_m &= -\sum_{n=2}^{\infty} 2^{n-2} f(n)\alpha_n[\lambda_m^n + (\lambda_m^*)^n] \\ &= 2(a_m^2-b_m^2)\alpha_2 - 4a_m(a_m^2-3b_m^2)\alpha_3 \\ &-8(a_m^4-6a_m^2b_m^2+b_m^4)\alpha_4 + 16a_m(a_m^4-10a_m^2b_m^2+5b_m^4)\alpha_5 \\ &+32(a_m^6-15a_m^4b_m^2+15a_m^2b_m^4-b_m^6)\alpha_6 - 64a_m(a_m^6-21a_m^4b_m^2 \\ &+35a_m^2b_m^4-7b_m^6)\alpha_7 + \cdots, \end{aligned}$$

and

$$\begin{aligned} y_m &= \frac{i}{b_m}\sum_{n=2}^{\infty} 2^{n-2} f(n)\alpha_n[\lambda_m^n - (\lambda_m^*)^n] \\ &= 4a_m\alpha_2 - 4(3a_m^2-b_m^2)\alpha_3 - 32a_m(a_m^2-b_m^2)\alpha_4 \\ &+16(5a_m^4-10a_m^2b_m^2+b_m^4)\alpha_5 + 64a_m(3a_m^4-10a_m^2b_m^2+3b_m^4)\alpha_6 \\ &-64(7a_m^6-35a_m^4b_m^2+21a_m^2b_m^4-b_m^6)\alpha_7 + \cdots, \end{aligned} \tag{18}$$

where $f(n)$ is as defined in Section 2. This represents a considerable generalisation of earlier results. It can be used to investigate behaviour in the complex λ_m planes. The remarkable point is that the nonlinear dynamics of soliton interactions and collisions can be specified by these rather simple compact formulae, even for systems that require very many terms for their description. If $\lambda_1 = \lambda_2$, then these coefficients reduce to the results found earlier in Section 3.3.

5 Soliton Superposition

Following the interpretation of parameters and specific loci on the complex plane, soliton superposition is a newly discovered phenomenon [10]. Here, in this work, we give explicit expressions for the locus plots, including their analytic solution for the first few operators. Nevertheless, it is possible to extend the results to an infinite number of operators in the hierarchy. From (18), we obtain the required locus plots by equating y_1 and y_2 for a given combination of α_j's. If we set $\alpha_2 = 1/2$ and leave α_5 arbitrary, with all other operator coefficients (α_3, α_4, α_6, α_7) set to zero, this form reduces to the known quintic two-soliton result (see [10], noting that $\delta = \alpha_5$). The velocity component of a soliton solution plays a central role in achieving soliton superposition. For a two-soliton solution, from (17), y_m is the velocity of soliton m, with $m=1, 2$. The explicit expression for this velocity component for the infinite hierarchy is given in (18). In the following sections, we describe the mechanism for soliton superposition for the first few operators.

5.1 NLSE

The NLSE is the first and fundamental operator in the infinite hierarchy, and it plays the lead role in terms of physical interpretation, as well as mathematical structure. For soliton superposition in the NLSE, firstly, we need to have a two-soliton solution with complex parameters. And this we can obtain from (17), with coefficient α_2 alone. We will mainly focus on the velocity component y_m, which is from (18), to achieve soliton superposition. The fundamental

criterion for soliton alignment follows from the relation $y_1=y_2$, where the velocity components involve complex parameters $\lambda_1=a_1+ib_1$ and $\lambda_2=a_2+ib_2$. The real parts, a_1, a_2, of the complex parameters, λ_1, λ_2, are responsible for the velocities of soliton 1 and soliton 2, respectively.

Now for NLSE, if we set the relation $y_1=y_2$, from (18), we have the simple relation $a_1=a_2$ to achieve soliton alignment. Interestingly, for the NLSE, soliton alignment is independent of the imaginary parts of the complex parameters, b_1 and b_2. As long as we keep the relation $a_1=a_2$, we will get aligned profiles of the two-soliton solution for each point on the complex plane. For example in the Figure 4, we get two aligned profiles for the same real parts, whereas the imaginary parts are different. To see the effect of variation of imaginary part of the complex parameter, we keep λ_2 fixed while changing λ_1. In Figure 4a, we have a crater shape in the vicinity of the two collision peak, with a low value of $b_1=0.6$ in the parameter λ_1. This crater shape becomes a chain shape with decreased frequency when b_1 and b_2 come closer to each other. For example, in Figure 4b, the chain shape forms with $b_1=1.1$ while $b_2=1.5$. However, we know that, if $\lambda_1=\lambda_2$, we will have a degenerate two-soliton solution and we do not have soliton superposition [17].

5.2 Hirota Equation

Unlike the NLSE, the next higher-order operator, which is the Hirota operator, possesses a more complicated mechanism for soliton superposition. In this case, soliton alignment can be presented on the complex plane. From (18), the velocity component for Hirota operator is

$$y_m=4[\alpha_2 a_m+\alpha_3(b_m^2-3a_m^2)].$$

So, setting $y_1=y_2$, we find, for any α_2:

$$b_1^2=3a_1^2-3a_2^2+b_2^2+\frac{\alpha_2}{\alpha_3}(a_2-a_1). \tag{19}$$

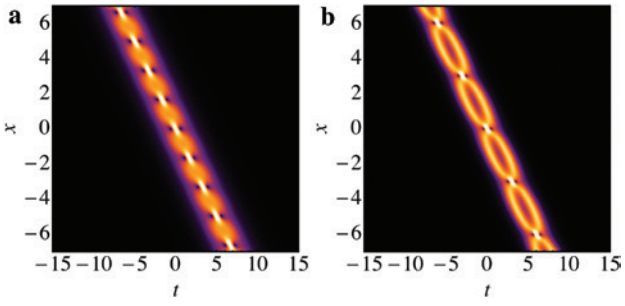

Figure 4: Examples of soliton superposition for the NLSE, with parameters (a) $\lambda_1=0.5+0.6i$ and $\lambda_2=0.5+1.5i$ and (b) $\lambda_1=0.5+1.1i$ and $\lambda_2=0.5+1.5i$ with $\alpha_2=1/2$.

If we plot these solutions, (19), for $\alpha_2=1/2$, we get the locus on the complex plane presented in Figures 5 and 7 for specific values of parameters λ_1, λ_2. Each point on these loci will give us aligned or superposed solitons with different patterns. However, we only consider the upper half of the complex plane indicated by the solution with positive values of b_1. In Figure 5, we keep parameter λ_1 arbitrary, whereas λ_2 is fixed. The red thick, dashed, and dotted lines are for varied values of $\alpha_3=1/3$, 1/9, and 1/13, respectively. With the decreased positive values of α_3, the loci shift their positions from left to right. The lower half (negative b_1) is symmetric and we disregard it for the moment. Although the alignment condition $y_1=y_2$ has been solved for b_1 for convenience, it can be solved for any arbitrary parameters, a_1, a_2, b_2. As a_1, a_2 control the soliton velocity, we again solve the soliton alignment condition numerically to find the exact value of a_1 for which two solitons are aligned. For $\lambda_1=a_1+i$ and $\lambda_2=1/2+i$ with $\alpha_3=1/2$, we get $a_1=-0.16667$ or 0.5. The 'magenta star' corresponds to $a_1=-0.16667$. Then $a_1=0.5$ corresponds to a value which give us a degenerate condition and so we disregard this value, as the solution will be indeterminate. To construct the locus plot Figure 5, we use a positive real part of λ_2, while keeping λ_1 positive. In general, with a positive real part, the soliton goes from right to left. However, in Figure 5, the 'magenta star' has a negative real part, so the aligned soliton goes from right to left; in other words, all the points on the locus in Figure 5 will give aligned solitons going from right to left, regardless of the signs of a_1, a_2 in the complex parameters. Examples of superposition are shown in Figure 6.

Similarly, in Figure 7, we use negative λ_2, whereas λ_1 is positive, and we get a different locus plot, providing different aligned structure of soliton superpositions.

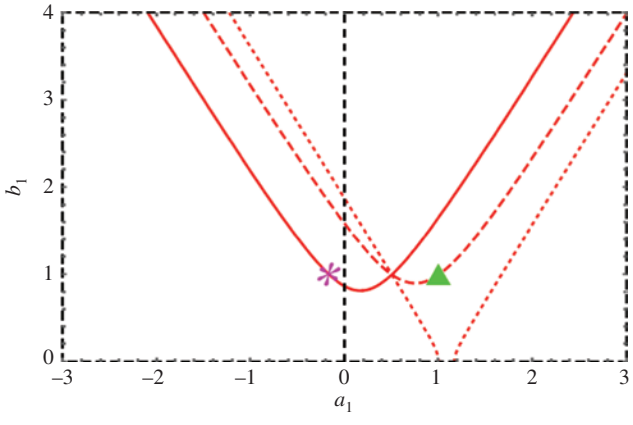

Figure 5: Locus plot from (19) for soliton superposition of Hirota equation for parameters $\lambda_2=1/2+i$ and $\lambda_1=a_1+ib_1$ while $\alpha_3=1/2$, 1/9, and 1/13.

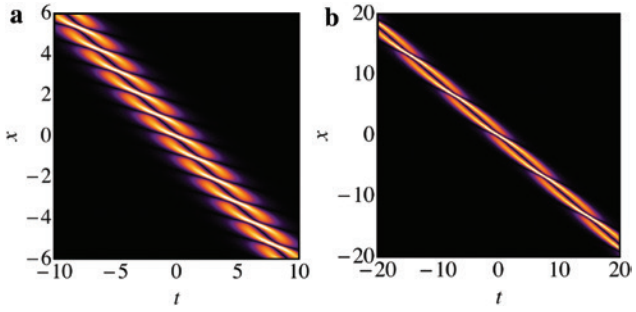

Figure 6: Examples of soliton superposition, from (19), for parameters (a) $\lambda_1=-0.16667+i$ and $\lambda_2=1/2+i$ (b) $\lambda_1=1.6667+i$ and $\lambda_2=1/2+i$ while $\alpha_3=1/13$.

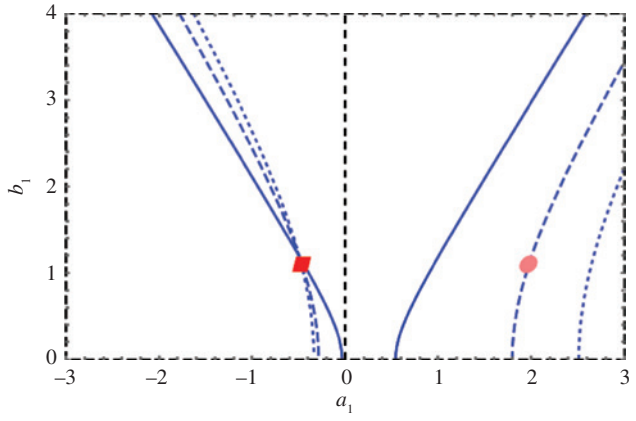

Figure 7: Locus plot, from (19), for parameters $\lambda_2=-1/2+1.2i$ and $\lambda_1=a_1+ib_1$ while $\alpha_3=1/3$, 1/9 and 1/13.

For example, the 'red square' and the 'pink circle' in Figure 7 give two different superposed structures. Regardless of the signs of the real parts of the parameters that control the velocities, including directions, both of the aligned pictures, Figure 8a,b, go from left to right. All the points on the locus in Figure 7 will give superposed solitons in same direction with basically these two types of structures with specific values of λ_1 and λ_2. A diverse range of structures can be obtained, depending on the ranges of the parameter values.

Now, if $\alpha_3=0$ and $\alpha_2\neq 0$, then there is no solution apart from $a_1=a_2$. When $\alpha_2\to 0$ and $\alpha_3\neq 0$ then, from (19):

$$b_1^2=3a_1^2-3a_2^2+b_2^2. \tag{20}$$

The expression is independent of α_3 and $b_1^2+3a_2^2=3a_1^2+b_2^2$, which is an ellipse. From (19) with $\alpha_2=1/2$, we use a positive value of b_1; this covers the upper half of the complex plane. From symmetry, a negative value of b_1 covers the lower half of the complex plane. Every point on the curve gives an aligned soliton and their structures fall into two categories, similar to Figure 8a,b, corresponding to either the 'red square' or the 'pink circle' in Figure 7. Examples of soliton superposition forms are shown in Figure 8.

5.3 LPD Equation

From (18), the velocity component for fourth-order operator or LPD equation can be given as

$$y_m=4a_m[\alpha_2+8(b_m^2-a_m^2)\alpha_4],$$

where $m=1$, 2 for soliton 1 and soliton 2, respectively, in the two-soliton solution. Now setting $y_1=y_2$, we get, for any α_2:

$$b_1^2=\frac{a_1^3-a_2^3+a_2b_2^2}{a_1}+\frac{\alpha_2}{8a_1\alpha_4}(a_2-a_1). \tag{21}$$

Figure 9 is the locus plot for soliton superposition in LPD equation, taking $\alpha_2=1/2$. We take parameters λ_1

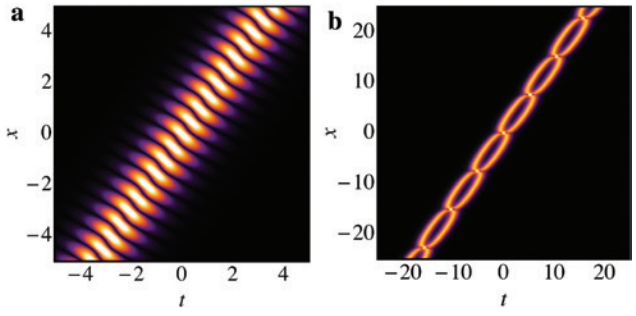

Figure 8: Examples of soliton superposition with parameters (a) $\lambda_1=-0.4689+1.1i$ and $\lambda_2=-1/2+1.2i$ (b) $\lambda_1=1.9689+1.1i$ and $\lambda_2=-1/2+1.2i$ while $\alpha_3=1/9$.

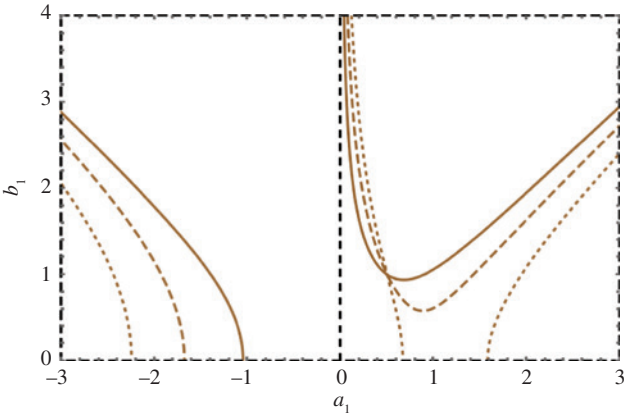

Figure 9: Locus plot, from (21), for parameters $\lambda_2=1/2+1.2$ and $\lambda_1=a_1+ib_1$ while $\alpha_4=1/8$, 1/32 and 1/64, indicated by solid, dashed, and with dotted lines, respectively.

arbitrary with $\lambda_2=1/2+i$, and plot results for parameter values $\alpha_4=1/8$, 1/32, and 1/64. All the points on these lines give superposed solitons with various structures. However, with the same parameters as those used in the Hirota case, the structures are mostly similar to the superposed structures of the Hirota equation. New types of structures are possible, depending on the particular ranges of parameter values. Now, if we use $\lambda_2=-1/2+i$ with $\lambda_1=a_1+ib_1$, we get a symmetric locus plot of Figure 9. This specific case is only valid for even-order operators. Below, for the quintic case, we will see that we get an asymmetric locus plot for $\pm a_m$ in λ_2 while λ_1 is arbitrary. This is also valid for the Hirota equation – note Figures 5 and 7.

Now with $\alpha_2=0$, while keeping $\alpha_4\neq 0$ and setting the velocity components to be equal, $y_1=y_2$, we get, from (21):

$$b_1^2=\frac{a_1^3-a_2^3+a_2b_2^2}{a_1}.$$

The locus plot of this expression resembles that of Figure 9, except that it is independent of α_4, and one can get similar superposed soliton structure as in Figure 8.

We can write a general expression for b_1, including the effects of α_2, α_3, and α_4. We find

$$b_1^2=\frac{F}{\alpha_3+8\alpha_4a_1}$$

where

$$F=8\alpha_4(a_1^3-a_2^3+a_2b_2^2)+\alpha_3(3a_1^2-3a_2^2+b_2^2)+\alpha_2(a_2-a_1), \tag{22}$$

assuming that α_3 and α_4 are not both zero. For example, (22) reduces to (21) when $\alpha_3=0$.

5.4 Quintic Equation

Now, the velocity component for the fifth-order operator or the quintic equation can be given as

$$y_m=4[a_m\alpha_2+4\alpha_5(5a_m^4-10a_m^2b_m^2+b_m^4)].$$

As we can see, this expression is a fourth-order polynomial. Therefore, setting $y_1=y_2$ will give us four solutions, in two pairs. In each pair of solutions, each is the complex conjugate of the other. Among the two pairs of solutions, one gives a locus on the upper half of the complex plane, whereas the other remains on the lower half. As we explained earlier, we will keep only the solutions that represent loci on the upper half of the complex plane. Nevertheless, both pairs are symmetric.

Now, setting $y_1=y_2$, we have, for any α_2:

$$b_1^2=5a_1^2\pm\frac{1}{2}\sqrt{4(20a_1^4+5a_2^4-10a_2^2b_2^2+b_2^4)+\frac{\alpha_2}{\alpha_5}(a_2-a_1)}. \tag{23}$$

In Figure 10, we take parameter $\lambda_2=1/2+i$, and in Figure 11, $\lambda_2=-1/2+i$, keeping $\lambda_1=a_1+ib_1$ arbitrary for both. The curves are for $\alpha_5=1/16$, 1/64, and 1/128 in both locus plots. In most cases, the structure of the superposed soliton on the locus plot resembles that of the superposed soliton in the Hirota case. However, infinitely many varieties can be possible as we change the parameter values. Two examples can be found in our previous work [10].

Now if we take $\alpha_2=0$ and set $y_1=y_2$, we have, from (23),

$$b_1^2=5a_1^2\pm\sqrt{20a_1^4+5a_2^4-10a_2^2b_2^2+b_2^4}. \tag{24}$$

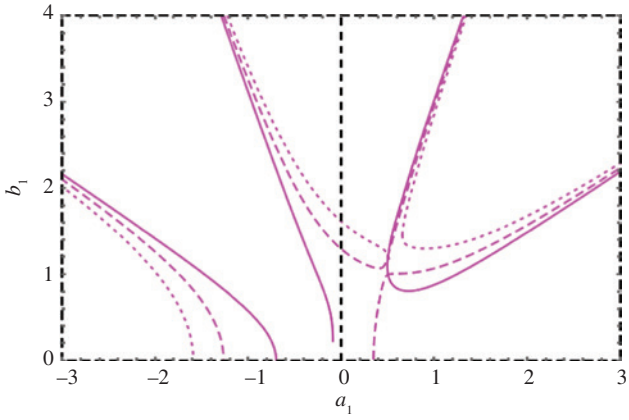

Figure 10: Locus plot, from (23) with $\alpha_2=1/2$, for parameters $\lambda_2=1/2+i$ and $\lambda_1=a_1+ib_1$ while $\alpha_5=1/16$, 1/64 and 1/128 for the solid, dashed, and dotted lines, respectively.

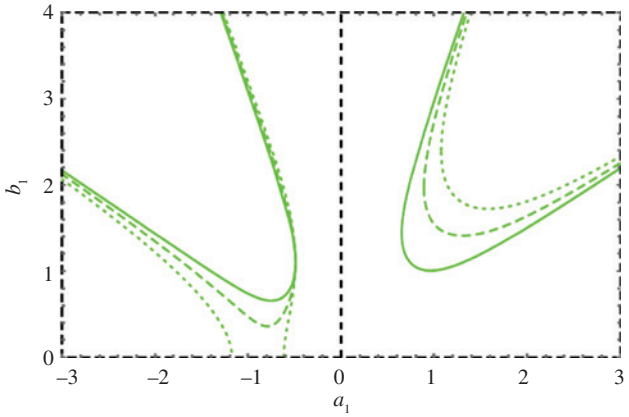

Figure 11: Locus plot, from (23) with $\alpha_2=1/2$, for parameters $\lambda_2=-1/2+i$ and $\lambda_1=a_1+ib_1$ while the solid, dashed, and dotted lines are for $\alpha_5=1/16$, 1/64, and 1/128, respectively.

This expression is independent of α_5. A representative locus plot is depicted in Figure 12. Interestingly, negative values of a_2 do not change the locus plot; this is quite obvious, since it has even powers in the polynomial.

5.5 Sextic Equation

Now, if α_6 is the only nonzero α_j, then we can factor as follows:

$$\frac{y_1}{192a_1\alpha_6}=(b_1^2-5a_1^2/3)^2-\frac{16}{9}a_1^4,$$

and so still obtain a simple form for b_1:

$$b_1^2=\frac{5a_1^2}{3}\pm\frac{1}{3}\sqrt{\frac{16a_1^5+9a_2^5-30a_2^3b_2^2+9a_2b_2^4}{a_1}}$$

6 Possible Extension to Sasa-Satsuma Equation

It may be possible to extend the approach presented here to the Sasa-Satsuma equation [8, 18–20]. It contains similar terms to those in the above-mentioned Hirota equation. Perturbations on both of these have been studied [9].

7 Conclusion

We have studied the propagation and superposition of solitons in systems governed by higher-order nonlinear Schrödinger-type equations. Such equations can have any number of operators contained within them. This allows for inclusion of subtle higher-order physical effects in fibres, oceanic waves, and superposed waves in BECs. We have given formulae for complex parameter pulses and also given conditions for soliton copropagation.

Acknowledgements: A. Ankiewicz acknowledges the support of the Australian Research Council (Discovery Project number DP140100265) and the Volkswagen Stiftung. A. Chowdury acknowledges Endeavour Postgraduate Award support.

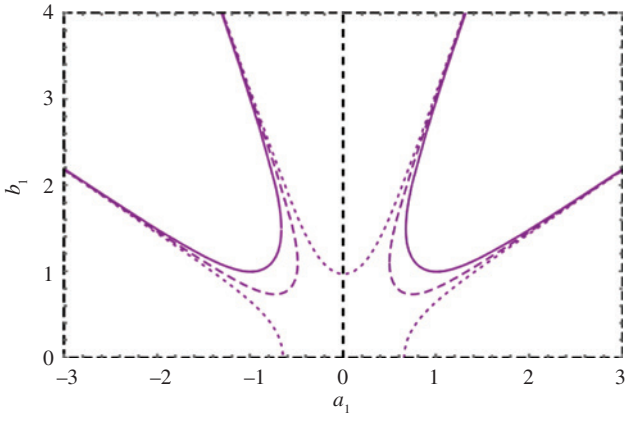

Figure 12: Locus plot, from (24), for parameters $\lambda_2=1+i$ is for the solid, $\lambda_2=1/2+i$ is for the dashed, and $\lambda_2=1/10+i$ is for the dotted line while $\lambda_1=a_1+ib_1$ is arbitrary.

Appendix

The coefficients for Section (4) are

$$\Omega_m(x,t)=a_mt+x(k_m+4a_mw_m), \tag{25}$$

and

$$\Theta_m(x,t)=b_mt+x\left(\frac{h_m}{2}+4b_mv_m\right). \tag{26}$$

Now, the terms can be expressed directly in terms of the parameters, λ_m, and their conjugates, λ_m^*.

For these (25) and (26), the (real) coefficients relevant to even order operators are

$$\begin{aligned}k_m&=-\sum_{j=1}^{\infty}2^{2j-2}\alpha_{2j}(-1)^j[\lambda_m^{2j}+(\lambda_m^*)^{2j}]\\&=2\alpha_2(a_m^2-b_m^2)-8\alpha_4(a_m^4-6a_m^2b_m^2+b_m^4)\\&+32\alpha_6(a_m^6-15a_m^4b_m^2+15a_m^2b_m^4-b_m^6)\\&-128\alpha_8(a_m^8-28a_m^6b_m^2+70a_m^4b_m^4-28a_m^2b_m^6+b_m^8)+\cdots,\end{aligned} \tag{27}$$

and

$$\begin{aligned}h_m&=i\sum_{j=1}^{\infty}2^{2j-1}\alpha_{2j}(-1)^j[\lambda_m^{2j}-(\lambda_m^*)^{2j}]\\&=8a_mb_m[\alpha_2-8\alpha_4(a_m^2-b_m^2)+16\alpha_6(3a_m^4-10a_m^2b_m^2+3b_m^4)\\&-256\alpha_8(a_m^6-7a_m^4b_m^2+7a_m^2b_m^4-b_m^6)+256\alpha_{10}(5a_m^8-60a_m^6b_m^2\\&+126a_m^4b_m^4-60a_m^2b_m^6+5b_m^8)+\cdots]\end{aligned} \tag{28}$$

The (real) coefficients relevant to odd order operators are

$$\begin{aligned}w_m&=\frac{1}{a_m}\sum_{j=1}^{\infty}2^{2j-3}\alpha_{2j+1}(-1)^j[\lambda_m^{2j+1}+(\lambda_m^*)^{2j+1}]\\&=-(a_m^2-3b_m^2)\alpha_3+4\alpha_5(a_m^4-10a_m^2b_m^2+5b_m^4)\\&-16\alpha_7(a_m^6-21a_m^4b_m^2+35a_m^2b_m^4-7b_m^6)+\cdots,\end{aligned} \tag{29}$$

and

$$v_m = -\frac{i}{b_m}\sum_{j=1}^{\infty} 2^{2j-3}\alpha_{2j+1}(-1)^j[\lambda_m^{2j+1} - (\lambda_m^*)^{2j+1}]$$
$$= -(3a_m^2 - b_m^2)\alpha_3 + 4\alpha_5(5a_m^4 - 10a_m^2 b_m^2 + b_m^4)$$
$$-16\alpha_7(7a_m^6 - 35a_m^4 b_m^2 + 21a_m^2 b_m^4 - b_m^6) + \cdots. \quad (30)$$

References

[1] N. Akhmediev and A. Ankiewicz, Solitons, Nonlinear Pulses and Beams, Chapman and Hall, London 1997; see chap.3, esp. eq.3.63.

[2] N. Akhmediev and A. Ankiewicz, Optics Commun. **100**, 186 (1993).

[3] C. Hamner, J. J. Chang, P. Engels, and M. A. Hoefer, Phys. Rev. Lett. **106**, 065302 (2011).

[4] B. Kibler, J. Fatome, C. Finot, G. Millot, G. Genty, et al., Sci. Rep. **2**, 463 (2012).

[5] B. Frisquet, B. Kibler, and G. Millot, Phys. Rev. X **3**, 041032 (2013).

[6] A. Chabchoub, N. Hoffmann, M. Onorato, and N. Akhmediev, Phys. Rev. X **2**, 011015 (2012).

[7] A. Chowdury, A. Ankiewicz, and N. Akhmediev, Proc.Royal Soc. A **471**, 20150130 (2015).

[8] N. Sasa and J. Satsuma, J. Phys. Soc. Japan **60**, 409 (1991).

[9] A. Ankiewicz, J. M. Soto-Crespo, M. A. Chowdhury, and N. Akhmediev, J. Opt. Soc. Am. B **30**, 87 (2013).

[10] A. Chowdury, D. J. Kedziora, A. Ankiewicz, and N. Akhmediev, Phys. Rev. E **90**, 032922 (2014).

[11] A. Chowdury, D. J. Kedziora, A. Ankiewicz, and N. Akhmediev, Phys. Rev. E **91**, 022919 (2015).

[12] A. Chowdury, D. J. Kedziora, A. Ankiewicz, and N. Akhmediev, Phys. Rev. E **91**, 032928 (2015).

[13] W. Xiao-Min, L. Qiu-Yan, and L. Zai-Dong, Chin. Phys. B **22**, 050311 (2013).

[14] R. Radha and P. S. Vinayagam, Rom. Rep. Phys. **67**, 89 (2015).

[15] V. S. Bagnato, D. J. Frantzeskakis, P. G. Kevrekidis, B. A. Malomed, and D. Mihalache, Rom. Rep. Phys. **67**, 5 (2015).

[16] A. Ankiewicz, D. J. Kedziora, A. Chowdury, U. Bandelow, and N. Akhmediev, Phys. Rev. E **93**, 012206 (2016).

[17] A. Ankiewicz and N. Akhmediev, Phys. Lett. A **91**, 358, (2014).

[18] D. Mihalache, L. Torner, F. Moldoveanu, N.C. Panoiu, and N. Truta, J. Phys. A **26**, L757 (1993).

[19] D. Mihalache, L. Torner, F. Moldoveanu, N.-C. Panoiu, and N. Truta, Phys. Rev. E **48**, 4699 (1993).

[20] D. Mihalache, N.-C. Panoiu, F. Moldoveanu, and D.-M. Baboiu, J. Phys. A **27**, 6177 (1994).